

## Supporting Information

### Location of the Metal Atoms in Ce<sub>2</sub>@C<sub>78</sub> and Its Bis-silylated Derivative

Michio Yamada, Takatsugu Wakahara, Takahiro Tsuchiya, Yutaka Maeda, Masahiro Kako, Takeshi Akasaka,\* Kenji Yoza, Ernst Horn, Naomi Mizorogi, and Shigeru Nagase  
*Contribution from the Center for Tsukuba Advanced Research Alliance, University of Tsukuba, Tsukuba, Ibaraki 305-8577, Japan, Department of Chemistry, Tokyo Gakugei University, Koganei, Tokyo 184-8501, Japan, Bruker AXS, K. K., Yokohama, Kanagawa 221-0022, Japan, Department of Chemistry, Rikkyo University, Tokyo 171-8501, Japan, and Department of Theoretical and Computational Molecular Science, Institute for Molecular Science, Okazaki, Aichi 444-8585, Japan*

E Mail: akasaka@tara.tsukuba.ac.jp

### Table of Contents

- Figure S1. (a) HPLC profiles of the DMF extract containing cerium metallofullerenes (upper trace) and the isolated Ce<sub>2</sub>@C<sub>78</sub> (lower trace). (b) LD-TOF mass spectrum of the isolated Ce<sub>2</sub>@C<sub>78</sub>. S3
- Figure S2. Visible-NIR spectra of Ce<sub>2</sub>@C<sub>78</sub> (red) and La<sub>2</sub>@C<sub>78</sub> (blue) in CS<sub>2</sub> solution. S4
- Figure S3. (a) DPV and (b) CV of Ce<sub>2</sub>@C<sub>78</sub> in 1,2-dichlorobenzene containing 0.1 M (*n*-Bu)<sub>4</sub>NPF<sub>6</sub>. S4
- Figure S4. <sup>13</sup>C NMR spectra (125 MHz) of Ce<sub>2</sub>@C<sub>78</sub> in CS<sub>2</sub> at 283–303 K. A capillary containing acetone-*d*<sub>6</sub> was used as an internal lock. The relative integrated intensity ration of the lines marked with an open circle and a solid circle is 2:1. S5
- Figure S5. Detailed equations of Fermi contact and pseudocontact interections, where  $C = -6.827 \times 10^7$  was used for the calculation. S6
- Figure S6. Line fitting plot for all carbon atoms of Ce<sub>2</sub>@C<sub>78</sub>; chemical shift vs.  $T^{-1}$ . (●) Observed chemical shifts of Ce<sub>2</sub>@C<sub>78</sub>; (▲) extrapolated values ( $\delta_{\text{dia}}$ ) at  $T^{-1} = 0$  on the line fitting. The extrapolated values  $\delta_{\text{dia}}$  deviate significantly from the observed <sup>13</sup>C NMR pattern of La<sub>2</sub>@C<sub>78</sub>. S7
- Figure S7. Line fitting plot for all carbon atoms of Ce<sub>2</sub>@C<sub>78</sub>; chemical shift vs.  $T^{-2}$ . (●) Observed chemical shifts of Ce<sub>2</sub>@C<sub>78</sub>; (▲) extrapolated values ( $\delta_{\text{dia}}$ ) at  $T^{-2} = 0$  on the line fitting. The extrapolated values  $\delta_{\text{dia}}$  are in good agreement with the observed <sup>13</sup>C

- NMR pattern of  $\text{La}_2@C_{78}$ . S8
- Figure S8. HPLC profiles for (a) reaction mixture and (b) isolated **1**. Conditions: column, Buckyprep (4.6 mm  $\times$  250 mm i.d.); eluent, toluene 1.0 mL/min. S9
- Figure S9. MALDI-TOF mass spectrum of **1** in negative mode. S9
- Figure S10. Visible-NIR spectra of  $\text{Ce}_2@C_{78}$  (blue) and adduct **1** (red) in  $\text{CS}_2$  solution. S9
- Figure S11. (a) DPV and (b) CV of **1** in 1,2-dichlorobenzene containing 0.1 M (*n*-Bu) $_4$ NPF $_6$ . The peaks of **1** and  $\text{Ce}_2@C_{78}$  formed by retro-cycloaddition are marked as red and blue circles, respectively. S10
- Figure S12. Multiscan CV of **1** in 1,2-dichlorobenzene containing 0.1 M (*n*-Bu) $_4$ NPF $_6$ , for different potential windows: (top), 0.3 to  $-1.1$  V (bottom) 1.1 to  $-1.1$  V. The peaks of **1** and  $\text{Ce}_2@C_{78}$  formed by retro-cycloaddition are marked as red and circles (blue arrows), respectively. S10
- Figure S13. HPLC profiles of **1**: (a) before CV, (b) after CV (bottom). Conditions: column, Buckyprep (4.6 mm  $\times$  250 mm i.d.); eluent, toluene 1.0 mL/min. S11
- Table S1. Redox Potentials of  $\text{Ce}_2@C_{78}$  and **1** S11
- Figure S14.  $^1\text{H}$  NMR spectra (300 MHz) of **1** in  $\text{CS}_2/\text{CD}_2\text{Cl}_2$  (3/1) at 198–288 K. S12
- Figure S15. Line fitting plot for all proton atoms of **1**; chemical shift vs.  $T^{-1}$ . (●) Observed chemical shifts of **1**; (▲) extrapolated values ( $\delta_{\text{dia}}$ ) at  $T^{-1} = 0$  on the line fitting. S13
- Figure S16. Line fitting plot for all proton atoms of **1**; chemical shift vs.  $T^2$ . (●) Observed chemical shifts of **1**; (▲) extrapolated values ( $\delta_{\text{dia}}$ ) at  $T^2 = 0$  on the line fitting. S14
- Figure S17.  $^{13}\text{C}$  NMR spectra (125 MHz) of **1** in  $\text{CS}_2/\text{CD}_2\text{Cl}_2$  (3/1) at 284–303 K. The signals marked by blue and green solid circles are due to the  $\text{sp}^2$ -carbon atoms and  $\text{sp}^3$ -carbon atoms on the cage, respectively. The signals marked by orange, yellow, pink, and light blue solid circles are due to the quaternary carbon atoms, CH carbon atoms, methylene carbon atom, and methyl carbon atoms on the mesityl group, respectively. S15
- Figure S18. Line fitting plot for all carbon atoms of **1**; chemical shift vs.  $T^{-1}$ . (●) Observed chemical shifts of **1**; (▲) extrapolated values ( $\delta_{\text{dia}}$ ) at  $T^{-1} = 0$  on the line fitting. S16
- Figure S19. Line fitting plot for all carbon atoms of **1**; chemical shift vs.  $T^2$ . (●)

Observed chemical shifts of **1**; ( $\blacktriangle$ ) extrapolated values ( $\delta_{\text{dia}}$ ) at  $T^{-1} = 0$  on the line fitting. S16

Table S2. Summary of Crystallographic Data of **1** at 130, 200, and 270 K S17

Figure S20. (a) Numbering diagram of a side view of **1**. S18

Figure S20. (b) Numbering diagram of another side view of **1**. S19

Figure S20. (c) Numbering diagram of the top view of **1**. The Ce atoms and the  $C_{78}$  cage except for C4, C17, C19, C29, C28, and C58 are omitted for clarity. S20

Figure S21. Packing diagrams of (a) wire frame and (b) space filling models in the crystal of **1**·2.5( $CS_2$ ) at 130 K. S21

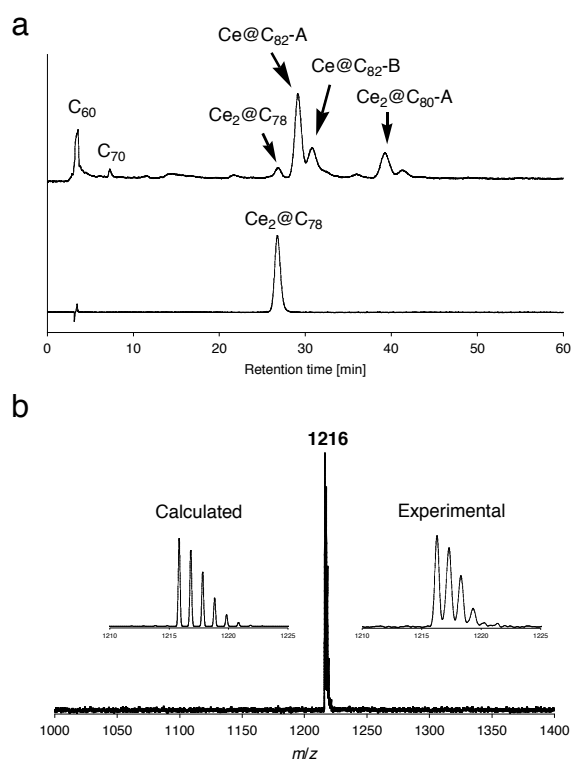


Figure S1. (a) HPLC profiles of the DMF extract containing cerium metallofullerenes (upper trace) and the isolated Ce<sub>2</sub>@C<sub>78</sub> (lower trace). Conditions: column, Buckyprep (4.6 mm × 250 mm i.d.); eluent, toluene 1.0 mL/min. (b) LD-TOF mass spectrum of the isolated Ce<sub>2</sub>@C<sub>78</sub>. The insets show the experimental and calculated isotope distributions of Ce<sub>2</sub>@C<sub>78</sub>.

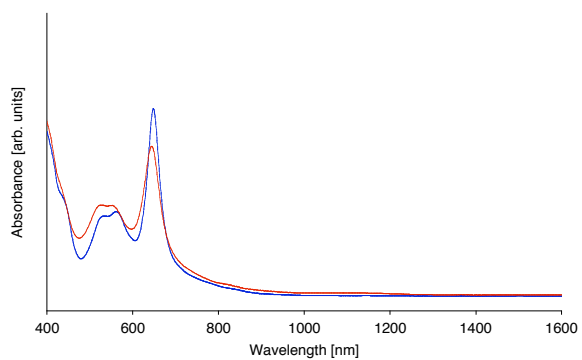


Figure S2. Visible-NIR spectra of  $\text{Ce}_2@C_{78}$  (red) and  $\text{La}_2@C_{78}$  (blue) in  $\text{CS}_2$  solution.

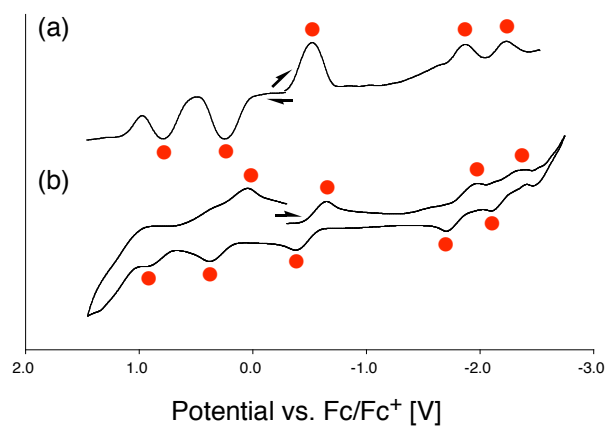


Figure S3. (a) DPV and (b) CV of  $\text{Ce}_2@C_{78}$  in 1,2-dichlorobenzene containing 0.1 M (*n*-Bu) $_4$ NPF $_6$ .

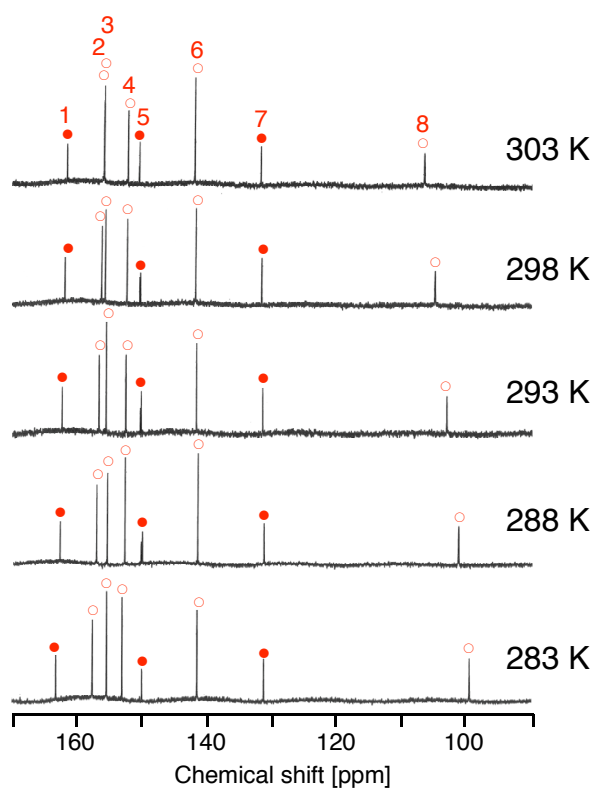
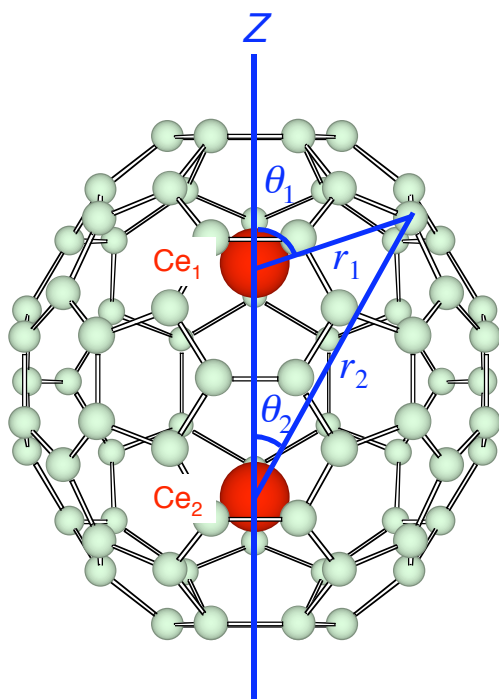


Figure S4.  $^{13}\text{C}$  NMR spectra (125 MHz) of  $\text{Ce}_2@C_{78}$  in  $\text{CS}_2$  at 283–303 K. A capillary containing acetone- $d_6$  was used as an internal lock. The relative integrated intensity ratio of the lines marked with an open circle and a solid circle is 2:1.



$$\delta_{fc} = \left( \frac{A_F g_J (g_J - 1) J(J+1) \mu_B}{3 \hbar \gamma_I k} \frac{1}{T} \right)_{M=Ce_1} + \left( \frac{A_F g_J (g_J - 1) J(J+1) \mu_B}{3 \hbar \gamma_I k} \frac{1}{T} \right)_{M=Ce_2}$$

$$\delta_{pc} = \left( C \frac{(3 \cos^2 \theta - 1)}{r^3} \frac{1}{T^2} \right)_{M=Ce_1} + \left( C \frac{(3 \cos^2 \theta - 1)}{r^3} \frac{1}{T^2} \right)_{M=Ce_2}$$

$$= \left( C \frac{(3 \cos^2 \theta_1 - 1)}{r_1^3} + C \frac{(3 \cos^2 \theta_2 - 1)}{r_2^3} \right) \frac{1}{T^2}$$

$$C = - \frac{\mu_0 g_J^2 \mu_B^2 J(J+1)(2J-1)(2J+3) D_z}{4\pi 60 k^2}$$

- $A_F$  : hyperfine coupling constant
- $g_J$  : Lande  $g$  factor
- $J$  : total angular momentum of the  $Ce^{3+}$  ion
- $\mu_B$  : Bohr magneton
- $\gamma_I$  : gyromagnetic ratio of the nucleus
- $k$  : Boltzmann constant
- $C$  : Bleaney factor
- $\mu_0$  : vacuum permeability
- $D_z$  : principal value of  $z$ -direction of the  $D$ -tensor

Figure S5. Detailed equations of Fermi contact and pseudocontact interactions, where  $C = -6.827 \times 10^7$  was used for the calculation.<sup>ref</sup>

ref) M. Yamada, T. Wakahara, Y. Lian, T. Tsuchiya, T. Akasaka, M. Waelchli, N. Mizorogi, S. Nagase, K. M. Kadish, *J. Am. Chem. Soc.* **2006**, *128*, 1400–1401.

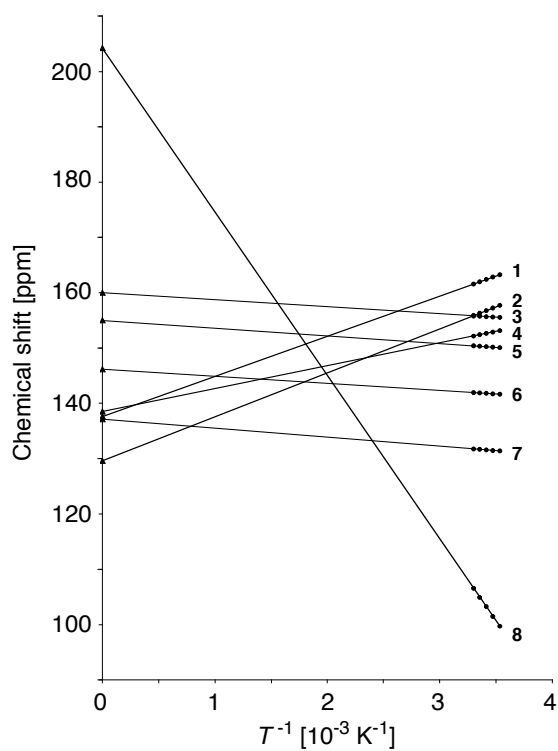


Figure S6. Line fitting plot for all carbon atoms of  $Ce_2@C_{78}$ ; chemical shift vs.  $T^{-1}$ . (●) Observed chemical shifts of  $Ce_2@C_{78}$ ; (▲) extrapolated values ( $\delta_{dia}$ ) at  $T^{-1} = 0$  on the line fitting. The extrapolated values  $\delta_{dia}$  deviate significantly from the observed  $^{13}C$  NMR pattern of  $La_2@C_{78}$ .

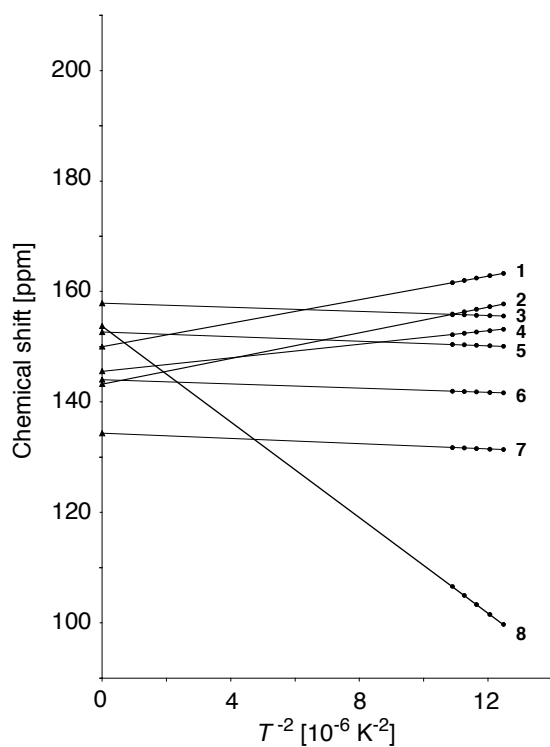


Figure S7. Line fitting plot for all carbon atoms of  $\text{Ce}_2@C_{78}$ ; chemical shift vs.  $T^{-2}$ . (●) Observed chemical shifts of  $\text{Ce}_2@C_{78}$ ; (▲) extrapolated values ( $\delta_{\text{dia}}$ ) at  $T^{-2} = 0$  on the line fitting. The extrapolated values  $\delta_{\text{dia}}$  are in good agreement with the observed  $^{13}\text{C}$  NMR pattern of  $\text{La}_2@C_{78}$ .

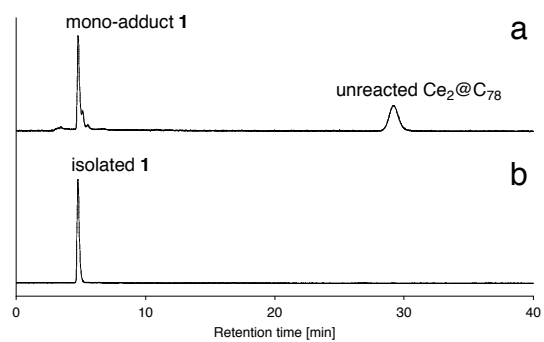


Figure S8. HPLC profiles for (a) reaction mixture and (b) isolated **1**. Conditions: column, Buckyprep (4.6 mm × 250 mm i.d.); eluent, toluene 1.0 mL/min.

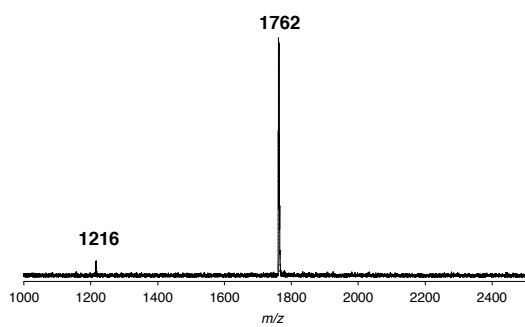


Figure S9. MALDI-TOF mass spectrum of **1** in negative mode.

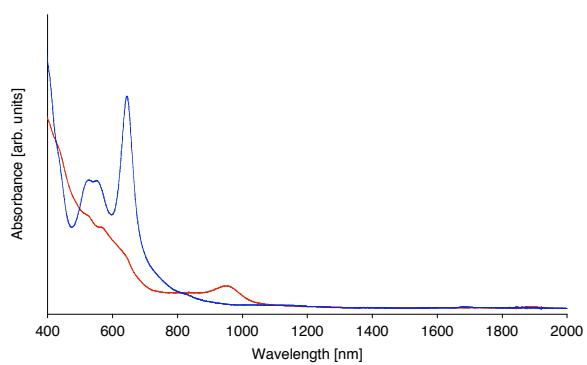


Figure S10. Visible-NIR spectra of Ce<sub>2</sub>@C<sub>78</sub> (blue) and **1** (red) in CS<sub>2</sub> solution.

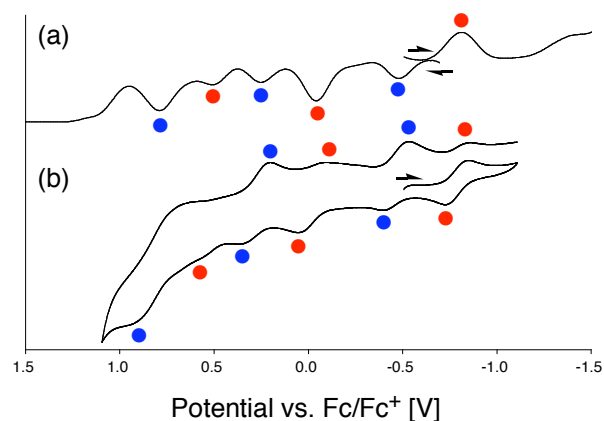


Figure S11. (a) DPV and (b) CV of **1** in 1,2-dichlorobenzene containing 0.1 M (*n*-Bu)<sub>4</sub>NPF<sub>6</sub>. The peaks of **1** and Ce<sub>2</sub>@C<sub>78</sub> formed by retro-cycloaddition are marked as red and blue circles, respectively.

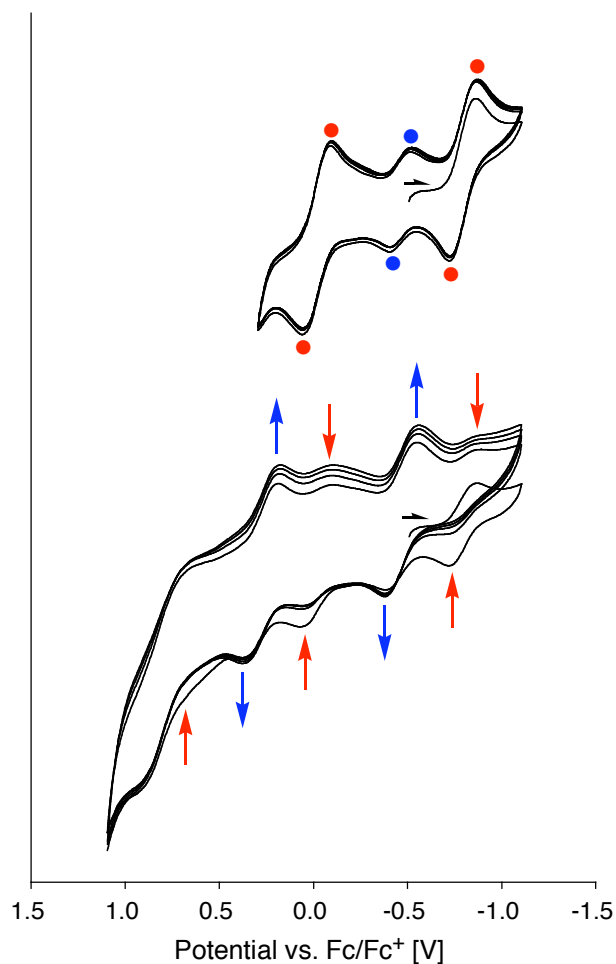


Figure S12. Multiscan CV of **1** in 1,2-dichlorobenzene containing 0.1 M (*n*-Bu)<sub>4</sub>NPF<sub>6</sub>, for different potential windows: (top) 0.3 to -1.1 V, (bottom) 1.1 to -1.1 V. The peaks of **1** and Ce<sub>2</sub>@C<sub>78</sub> formed by retro-cycloaddition are marked as red and circles (blue

arrows), respectively.

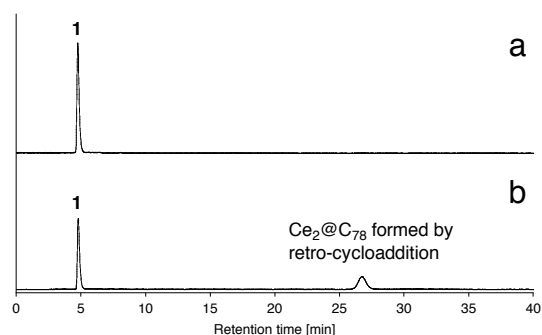


Figure S13. HPLC profiles of **1**: (a) before CV, (b) after CV (bottom). Conditions: column, Buckyrep (4.6 mm × 250 mm i.d.); eluent, toluene 1.0 mL/min.

Table S1. Redox Potentials<sup>a</sup> of Ce<sub>2</sub>@C<sub>78</sub> and **1**

Compd.	<sup>ox</sup> <i>E</i> <sub>2</sub>	<sup>ox</sup> <i>E</i> <sub>1</sub>	<sup>red</sup> <i>E</i> <sub>1</sub>	<sup>red</sup> <i>E</i> <sub>2</sub>	<sup>red</sup> <i>E</i> <sub>3</sub>
<b>1</b>	+0.50 <sup>b</sup>	-0.04	-0.81		
Ce <sub>2</sub> @C <sub>78</sub>	+0.79 <sup>b</sup>	+0.25	-0.52	-1.86	-2.23

<sup>a</sup>Values are obtained by differential pulse voltammetry in volts relative to ferrocene/ferrocenium couple. Conditions: 0.1 M (*n*-Bu)<sub>4</sub>NPF<sub>6</sub> in 1,2-dichlorobenzene; working electrode, Pt disk; counter electrode, Pt wire; reference electrode, SCE.

<sup>b</sup>Irreversible.

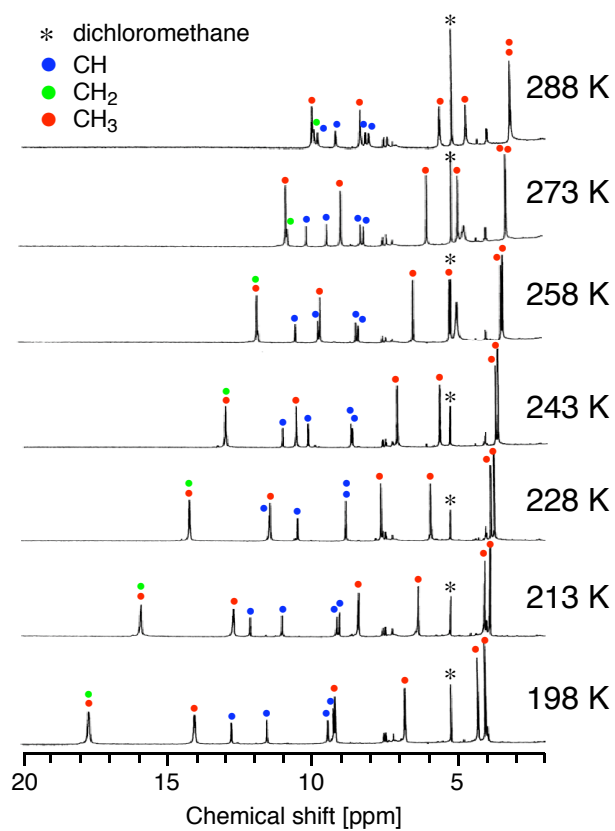


Figure S14. <sup>1</sup>H NMR spectra (300 MHz) of **1** in CS<sub>2</sub>/CD<sub>2</sub>Cl<sub>2</sub> (3/1) at 198–288 K.

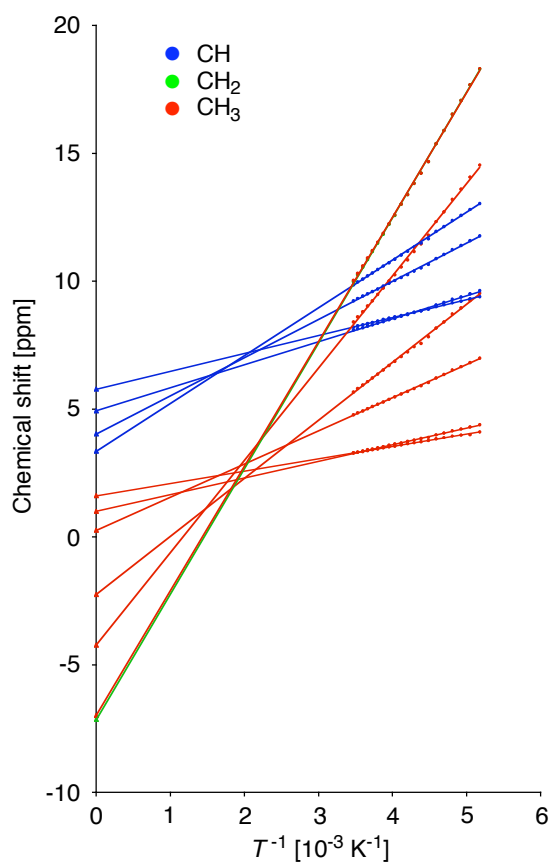


Figure S15. Line fitting plot for all proton atoms of **1**; chemical shift vs.  $T^{-1}$ . (●) Observed chemical shifts of **1**; (▲) extrapolated values ( $\delta_{\text{dia}}$ ) at  $T^{-1} = 0$  on the line fitting.

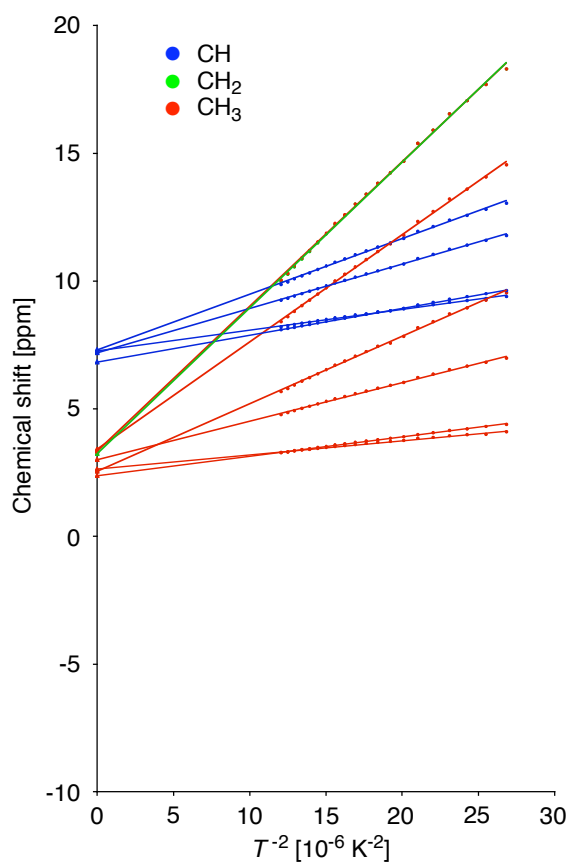


Figure S16. Line fitting plot for all proton atoms of **1**; chemical shift vs.  $T^{-2}$ . (●) Observed chemical shifts of **1**; (▲) extrapolated values ( $\delta_{\text{dia}}$ ) at  $T^{-2} = 0$  on the line fitting.

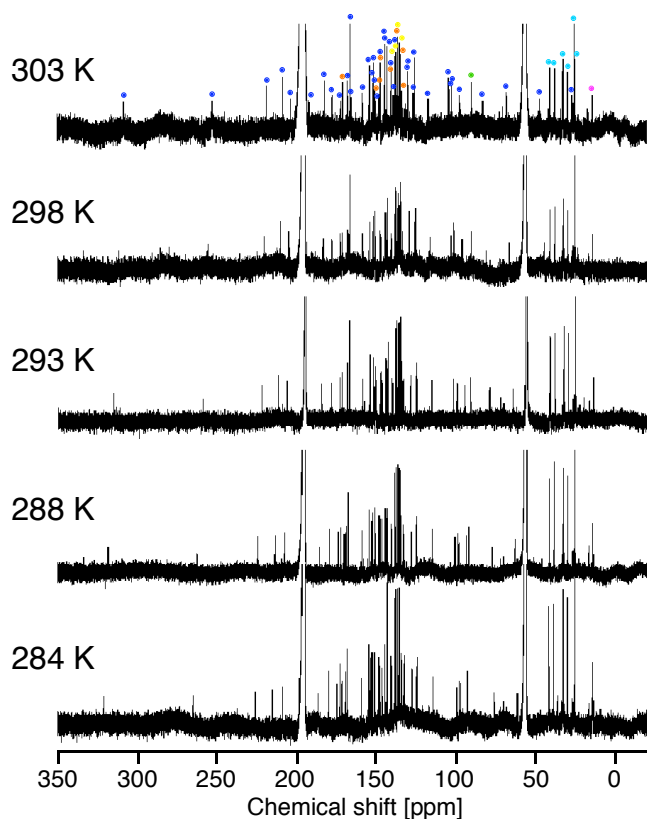


Figure S17.  $^{13}\text{C}$  NMR spectra (125 MHz) of **1** in  $\text{CS}_2/\text{CD}_2\text{Cl}_2$  (3/1) at 284–303 K. The signals marked by blue and green solid circles are due to the  $\text{sp}^2$ -carbon atoms and  $\text{sp}^3$ -carbon atoms on the cage, respectively. The signals marked by orange, yellow, pink, and light blue solid circles are due to the quaternary carbon atoms, CH carbon atoms, methylene carbon atom, and methyl carbon atoms on the mesityl group, respectively.

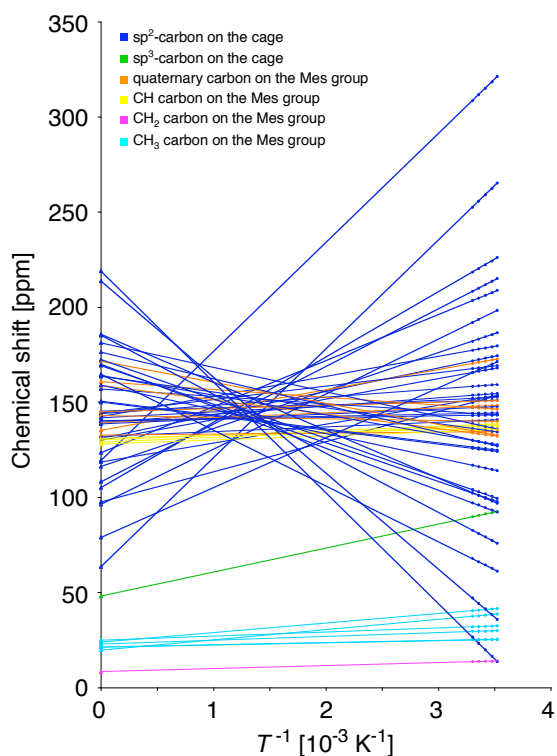


Figure S18. Line fitting plot for all carbon atoms of **1**; chemical shift vs.  $T^{-1}$ . (●) Observed chemical shifts of **1**; (▲) extrapolated values ( $\delta_{\text{dia}}$ ) at  $T^{-1} = 0$  on the line fitting.

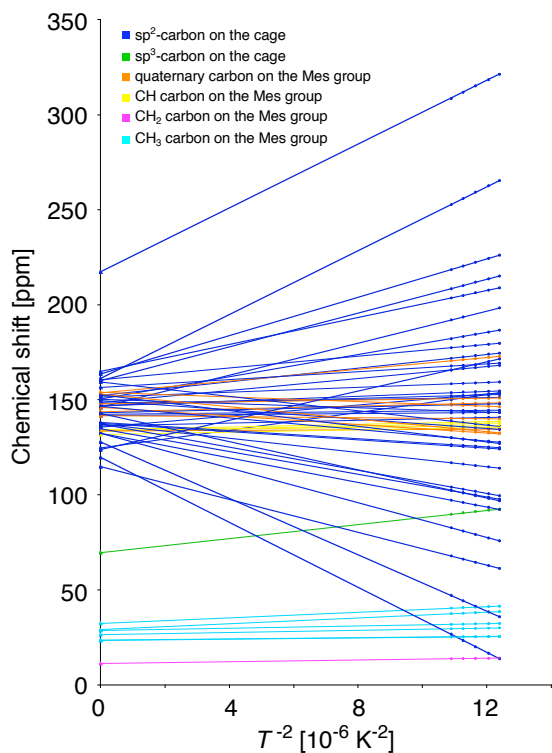


Figure S19. Line fitting plot for all carbon atoms of **1**; chemical shift vs.  $T^{-2}$ . (●) Observed chemical shifts of **1**; (▲) extrapolated values ( $\delta_{\text{dia}}$ ) at  $T^{-1} = 0$  on the line

fitting.

Table S2. Summary of Crystallographic Data of **1** at 130, 200, and 270 K

Temperature	130 K	200 K	270 K
Formula	C <sub>117.5</sub> H <sub>46</sub> Ce <sub>2</sub> S <sub>3</sub> Si <sub>2</sub>	C <sub>117.5</sub> H <sub>46</sub> Ce <sub>2</sub> S <sub>3</sub> Si <sub>2</sub>	C <sub>117.5</sub> H <sub>46</sub> Ce <sub>2</sub> S <sub>3</sub> Si <sub>2</sub>
formula weight	1954.26	1954.26	1954.26
wavelength, Å	0.68880	0.68880	0.68880
crystal system	Orthorhombic	Orthorhombic	Orthorhombic
space group	<i>P</i> 2 <sub>1</sub> 2 <sub>1</sub> 2 <sub>1</sub>	<i>P</i> 2 <sub>1</sub> 2 <sub>1</sub> 2 <sub>1</sub>	<i>P</i> 2 <sub>1</sub> 2 <sub>1</sub> 2 <sub>1</sub>
<i>a</i> , Å	11.300(2)	11.318(3)	11.351(3)
<i>b</i> , Å	23.437(4)	23.492(5)	23.560(5)
<i>c</i> , Å	27.993(6)	28.055(6)	28.117(7)
$\alpha$ , deg	90.00	90.00	90.00
$\beta$ , deg	90.00	90.00	90.00
$\gamma$ , deg	90.00	90.00	90.00
Volume, Å <sup>3</sup>	7414(2)	7459(3)	7519(3)
<i>Z</i>	4	4	4
<i>D</i> <sub>calc</sub> , Mg/m <sup>3</sup>	1.751	1.741	1.727
Absorption coefficient	1.449	1.441	1.429
<i>F</i> (000)	3900	3900	3900
$\theta$ range, deg	1.41 to 24.51	1.41 to 24.51	1.40 to 24.52
Limiting indices	-13 ≤ <i>h</i> ≤ 13 -18 ≤ <i>k</i> ≤ 18 -33 ≤ <i>l</i> ≤ 33	-13 ≤ <i>h</i> ≤ 13 -19 ≤ <i>k</i> ≤ 18 -33 ≤ <i>l</i> ≤ 33	-13 ≤ <i>h</i> ≤ 13 -18 ≤ <i>k</i> ≤ 19 -33 ≤ <i>l</i> ≤ 33
Reflections collected	34138	33749	34267
Independent reflections	10295	10233	10346
data / restraints / parameters	10295 / 977 / 1186	10233 / 977 / 1186	10346 / 977 / 1186
<i>R</i> <sub>int</sub>	0.0387	0.0370	0.0406
<i>R</i> <sub>1</sub> [ <i>I</i> > 2σ( <i>I</i> )]	0.0491	0.0465	0.0475
<i>wR</i> <sub>2</sub> [ <i>I</i> > 2σ( <i>I</i> )]	0.1365	0.1259	0.1294
<i>R</i> <sub>1</sub> [all data]	0.0582	0.0572	0.0587
<i>wR</i> <sub>2</sub> [all data]	0.1445	0.1332	0.1357
GOF on <i>F</i> <sup>2</sup>	1.035	1.007	1.037
max, min peaks, e/Å <sup>3</sup>	1.182, -0.975	0.749, -0.885	0.952, -0.944

(a)

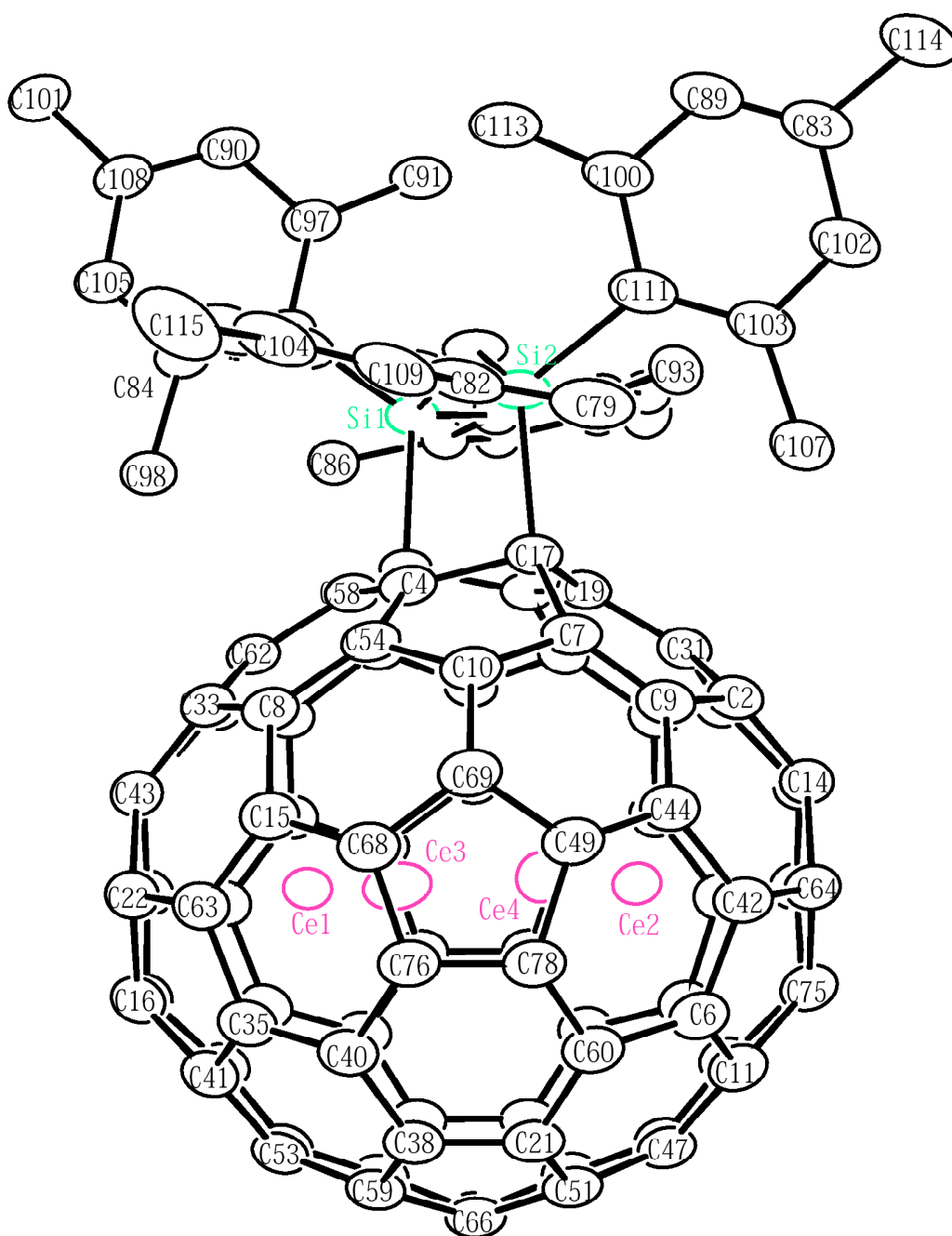


Figure S20. (a) Numbering diagram of a side view of **1**.

(b)

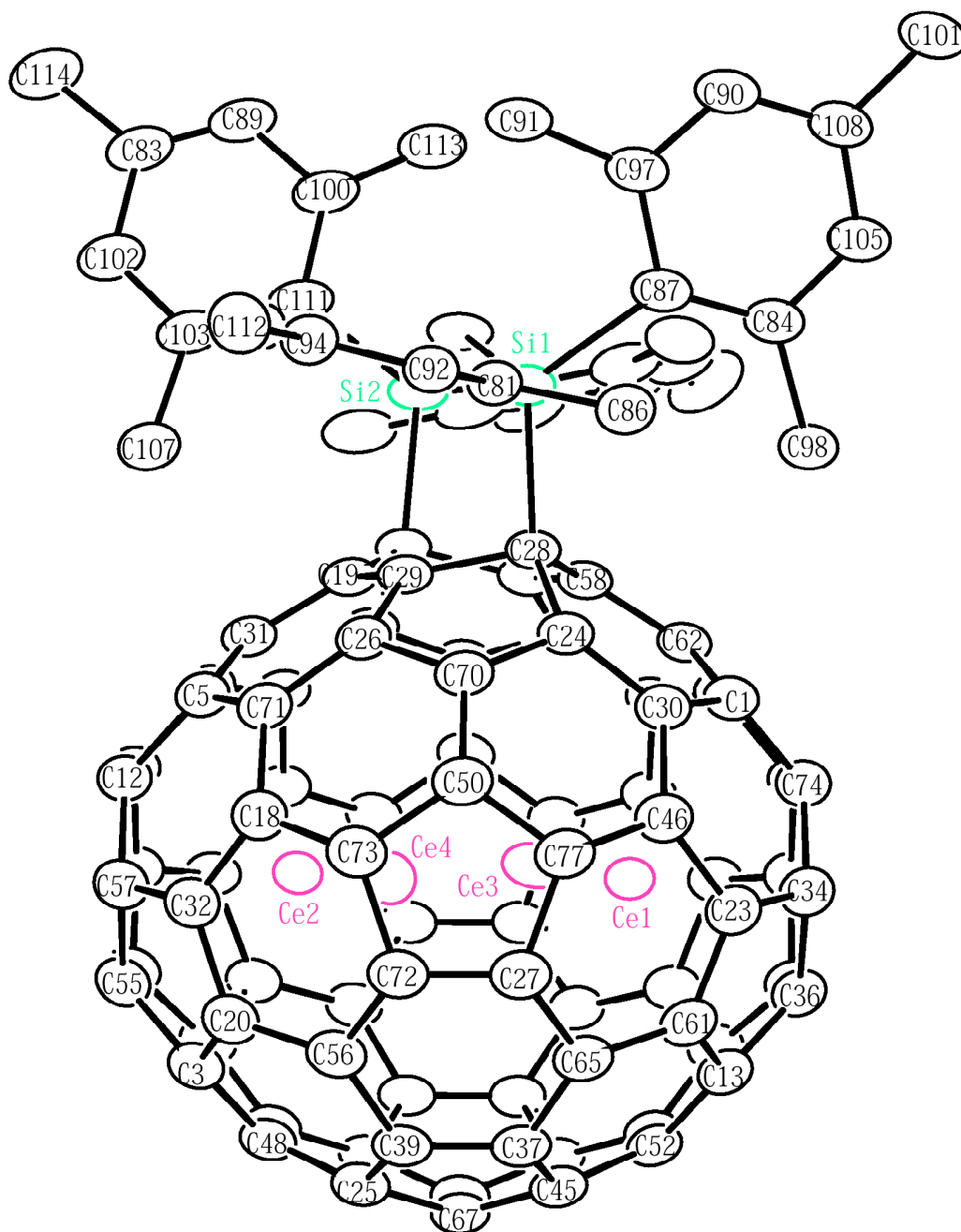


Figure S20. (b) Numbering diagram of another side view of **1**.

(c)

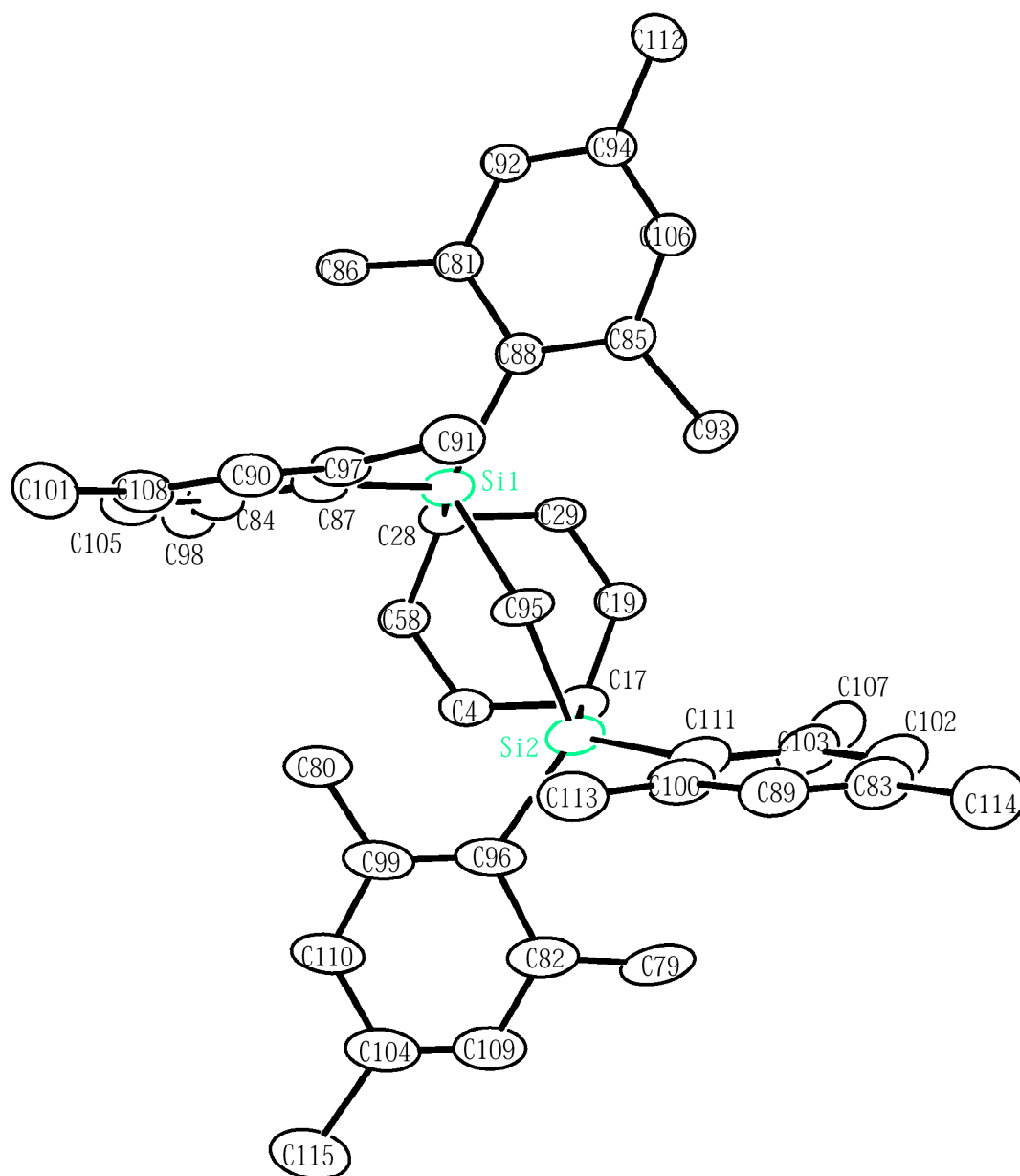
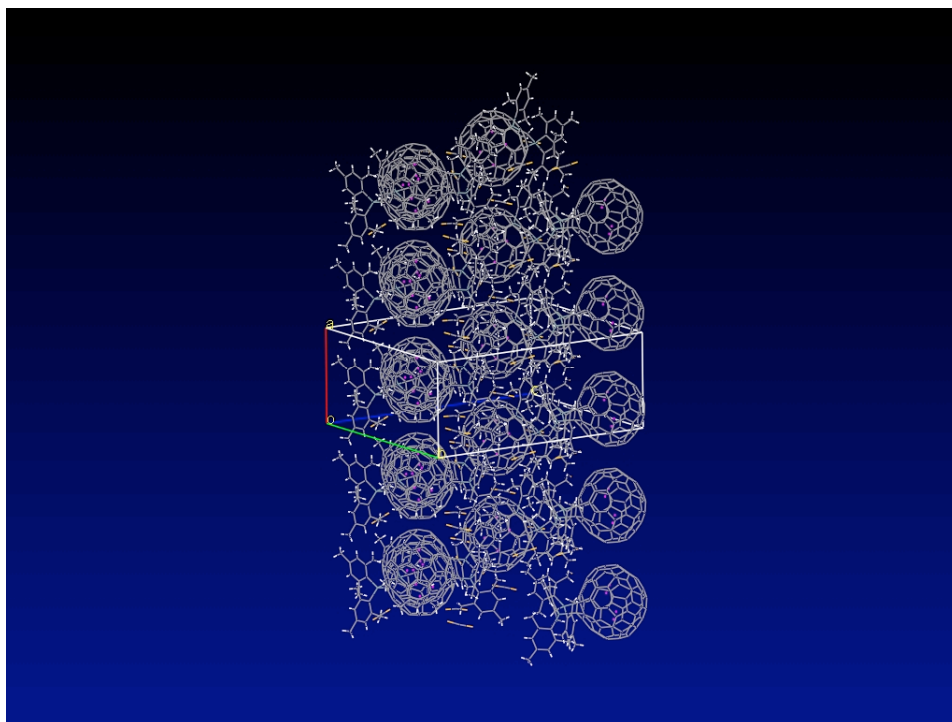


Figure S20. (c) Numbering diagram of the top view of **1**. The Ce atoms and the C<sub>78</sub> cage except for C4, C17, C19, C29, C28, and C58 are omitted for clarity.

(a)



(b)

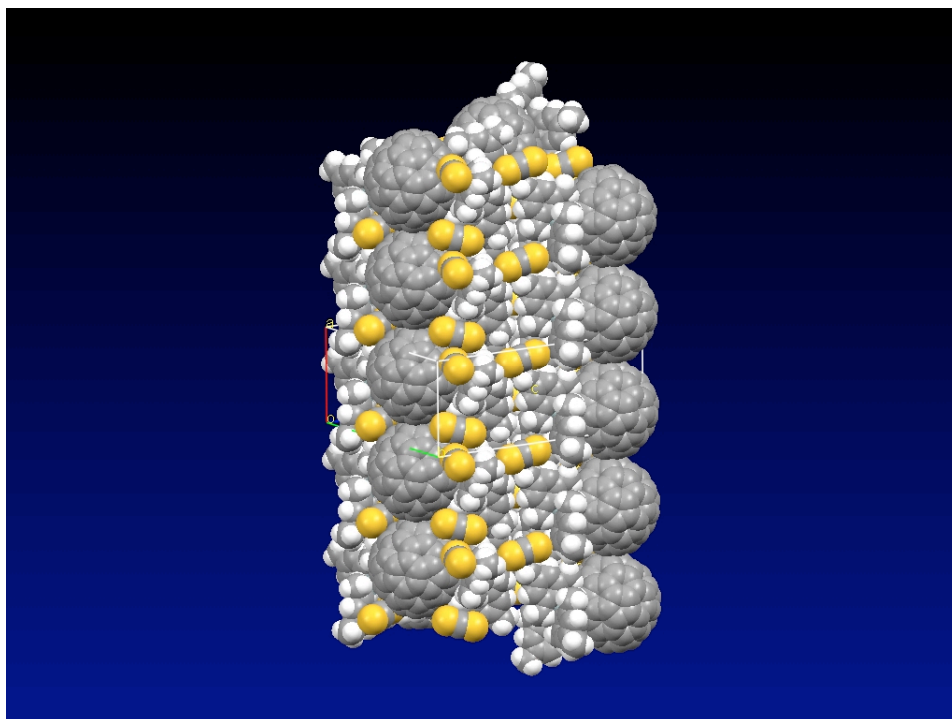


Figure S21. Packing diagrams of (a) wire frame and (b) space filling models in the crystal of 1·2.5(CS<sub>2</sub>) at 130 K.